

- \mathbf{M} is the 7x7 proper mass matrix of the device. This matrix contains coupling terms between the pendulum and the floating body and depends on the position vector and the velocity vector, as we did not assumed linearity. The calculation of \mathbf{M} is complex and is not the main point of this paper. Details and expression of \mathbf{M} as a function of the mechanical parameters of the device can be found in [2].
- \mathbf{F}_C is the Coriolis force. The expression of this force is given in [2].
- \mathbf{F}_{PTO} represents the action of the Power-Take-Off. It is modelled here as a linear damper, with B_{PTO} being the damping coefficient.
- \mathbf{F}_H represents the force due to the fluid-structure interactions.

Fluid-structure interactions

The following usual assumptions are made: the fluid is considered homogeneous, incompressible, inviscid and the flow irrotational. Surface tension is not taken into account, the depth is considered infinite and a linearized free surface and body boundary conditions are used. The fluid forces acting on the body can be non-linear with respect to certain motion variables, e.g the quadratic component of the Bernoulli's equation, the nonlinear incident potential flow. They contain "geometric" non-linearities as in the case where the force are computed by integrating on the exact instantaneous position and shape on the immersed part of the body. The first-order force is calculated by a linear potential flow formulation whereas the second-order force is calculated by adding the quadratic term of Bernoulli's equation and by expanding the first-order force to the second-order with the Taylor expansion

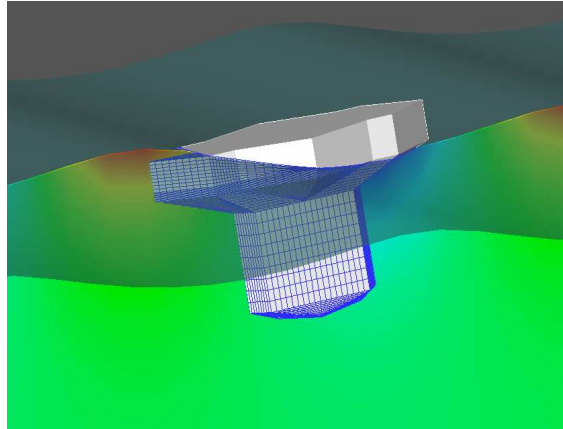


Figure 2 : 3D view of the SEAREV and its wetted surface.

Froude-Krylov forces

The integration of the incident wave pressure is performed over the instantaneous total wetted surface at each time step, taking into account the large motions of the ship and its exact intersection with the undisturbed wave surface. The Froude-Krylov force is expressed by:

$$f_{FK}(t) = \iint (p_S + p_D) n ds$$

Where the static and dynamic pressure are, respectively:

$$p_S = -\rho g z, \quad -\infty < z < \eta$$

$$p_D = -\rho \frac{\delta \phi_I}{\delta t}$$

The dynamic pressure is derived from the non-linear incident potential of a higher-order spectral method [8]. A robust geometry processing capability is essential for large amplitude motions. Consequently, an automatic remeshing routine was developed for this task. At each time step, the underwater geometry is represented by a number of panels. As the body moves, its new location and orientation is updated in the global coordinate system and the new waterline is found from the intersection with the instantaneous free surface. The underwater portion of each panel is then repanelized using the transfinite method [9] (Figure (2)).

Radiation forces

The linear radiation forces have been expressed as a convolution product according to the well-known Cummins' decomposition:

$$F_{rad}(t) = -\mu_{\infty} \dot{Y} - \int_0^t K(t-\tau) \dot{X}(\tau) d\tau$$

It can first be transformed in order to remove the convolution product by using Prony's method. This method has been implemented by Daubisse [5] and further developed by Clément [4] for the computation of impulse response of radiation forces

Diffraction forces

Like the radiation forces, the diffraction forces are based here on linear theory in the time domain. The diffracted wave forces are computed as:

$$F_{diff}(t) = \int_{-\infty}^{\infty} K_7(t-\tau) \eta_0(\tau) d\tau$$

where K_7 is the impulse response function for the diffraction forces and η_0 is the free surface elevation of the incident wave at a given reference point.

Expansion to the second-order.

The expansion to the second order is realized in two steps. In the first step, the linear hydrodynamic force is developed, using Taylor expansion in order to obtain:

$$F_{2nd}(t) = \iint_{C_0} \phi_t(t, M'_0) n'_0 dM'_0 + \iint_{C_0} \left[\partial x' \cdot \frac{\partial \phi_t(t, M'_0)}{\partial x'} + \partial y' \cdot \frac{\partial \phi_t(t, M'_0)}{\partial y'} + \partial z' \cdot \frac{\partial \phi_t(t, M'_0)}{\partial z'} \right] n'_0 dM'_0 + \iint_{C_0} \phi_t(t, M'_0) \partial n'_0 dM'_0$$

In the second step, the quadratic term of the Bernoulli's equation is taken into account by a convolution as the following:

$$F_{V^2/2}(t) = -\frac{\rho}{2} \iint_{C_0} |\nabla \phi \cdot \dot{X}|^2 n_0 dS - \frac{\rho}{2} \iint_{C_0} |\nabla \phi \cdot V_I|^2 n_0 dS$$

where C_0 is the mean wetted surface, V_I is the incident wave. Terms from second-order radiation and diffraction potentials were ignored in this study.

VALIDATION

We considered a truncated circular cylinder of radius 1 meter in infinite water depth. The mean drift forces on the cylinder are showed on the figure (3). The forces are normalized by gR_0A^2 where ρ is the water density, g is the gravitational acceleration, R_0 is the radius and A is the wave amplitude. K is the infinite depth wave number. The plot on the figure (3) shows surge forces computed by two different approaches; the analytic solution (Molin [6]) and the model presented in this paper. The figure (3) shows that the numerical model underestimates the mean surge force in the low wave number range.

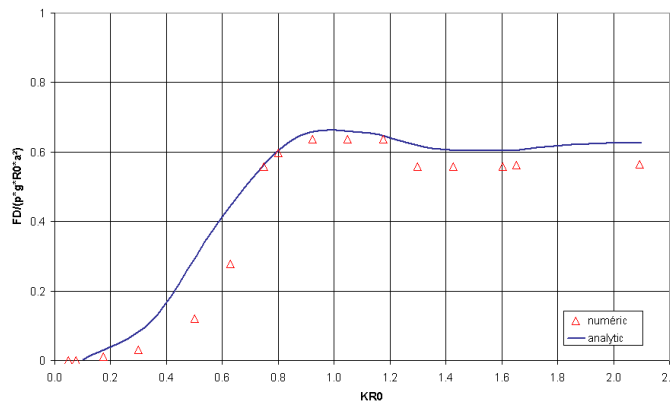


Figure 3 : Nonlinear mean surge forces on a cylinder.

Correlation between numerical and experimental results.

Experiments with 1/12-scale model of the SEAREV body were conducted in ECN's ocean engineering basin [7]. In order to compare the experimental results against the numerical model solutions, all the results were condensed in the form of transfer functions. Figure (5) shows a comparison between the non-linear formulation, a linear time domain formulation [2] and experimental results for a regular wave train with 0,083 meter of amplitude and with frequency is the range between 0,4 and 0,64 Hz. A fair agreement between theory and experiments is thus obtained. Figure (4) shows that a good prediction of the behaviour of the SEAREV device is obtained. The dynamic of the system is correctly recovered even if the motion amplitudes are slightly overestimated.

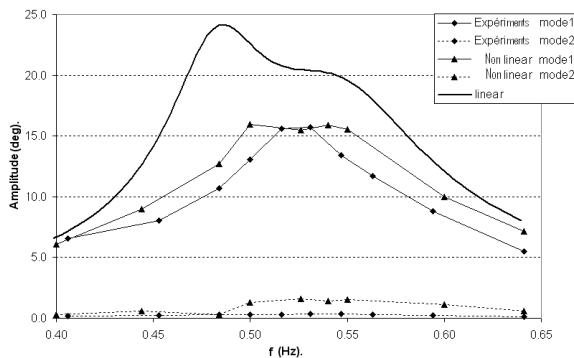


Figure 5: RAO for the pitch motion of the SEAREV device. Comparison between experiments and numerical simulation.

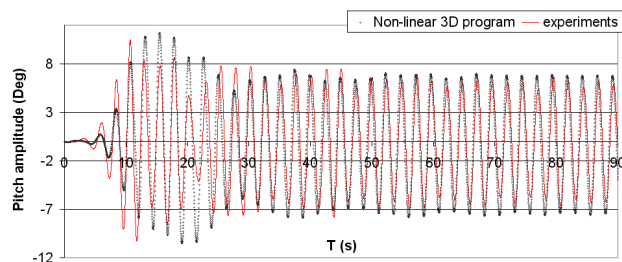


Figure 4: Pitch angle as a function of time. Comparison between experiments and numerical simulation.

CONCLUSION

We have presented in this paper a numerical model to determine the large amplitude motions of a floating wave energy converter subjected to incoming regular waves. The numerically motions of the body in regular waves, were compared with experimental results. The results predicted by the model agree reasonable well with experimental results.

Acknowledgments

This work is a result of research sponsored in part by ADEME, Agence de l'environnement et de la Maîtrise de l'Énergie.

REFERENCES

- [1] Robert H. Bracewell. Frog and PS Frog (1990), A Study of Two Reactionless Ocean Wave Energy Converters. PhD thesis, Lancaster University.
- [2] Babarit A., Optimisation Hydrodynamique et Contrôle Optimal d'un Récupérateur de l'Énergie des Vagues. PhD thesis (2005), Ecole Centrale de Nantes, in French.
- [3] Babarit A., Clément A.H. , Gilloteaux J-C, Josset C. & Duclos G. (2005), The SEAREV Wave Energy Converter, 6 European Wave & Tidal Energy Conference.
- [4] Clément A.H (1999), Using differential properties of the Green function in seakeeping computational codes. Proc. 7th Intern. Conf. Numer. Ship Hydrol., 6(5):1–15.
- [5] Daubisse J-C (1981), Some results on approximation by exponential series applied to hydrodynamics. Proc. 3rd Intern. Conf. Numer. Ship Hydrol., Paris.
- [6] Molin B., Hydrodynamique des structures offshore, Edition TECHNIP.
- [7] Durand M. Babarit A., Pettinotti B., Quillard O., Toularastel J.L. and Clément A.H (2007), Experimental validation of the performance SEAREV wave energy converter with real time latching control, EWTEC, Porto.
- [8] Ducrozet G., Bonnefoy F., Le Touzé D. and Ferrant P. (2006), Development of a fully nonlinear water wave simulator based on higher order spectral theory, 20th Workshop on Water Waves and Floating Bodies, Norway.
- [9] Coons S.A. (1987), Méthode matricielle, Hermès.